

Strain-stabilized precursor clusters in potassium thiocyanate

O. Blaschko,* W. Schranz, M. Fally, G. Krexner, and Z. Łodziana†
Institut für Experimentalphysik, Universität Wien, Strudlhofgasse 4, A-1090 Wien, Austria
 (Received 27 May 1998)

We present refined diffuse neutron scattering measurements performed in the long-range-ordered phase of potassium thiocyanate ($T < T_c$). The analysis of the data yields that the diffuse scattering is due to the presence of order-parameter fluctuations that appear as a precursor to the order-disorder phase transition. The diffuse intensity increases when approaching T_c from below, whereas the width remains constant in the whole long-range-ordered phase. Molecular-dynamics simulations indicate that the size of the precursor clusters is stabilized by the order-parameter-strain interactions. [S0163-1829(98)06537-0]

I. INTRODUCTION

Several molecular crystals of the thiocyanate family, e.g., MSCN ($M = \text{K, Rb, NH}_4, \text{TI, } \dots$), exhibit an order-disorder phase transition (PT) related to the reorientation of the linear SCN molecules.¹ At T_c this reorientation leads to a structural change from an orthorhombic phase ($Pbcm-D_{2h}^{11}$, $Z=4$) to a tetragonal phase ($I4/mcm-D_{4h}^{18}$, $Z=2$). The transition temperatures are $T_c^K = 415$ K and $T_c^{\text{Rb}} = 435$ K for KSCN and RbSCN, respectively.

In both cases the phase transition is of first order.² According to birefringence³ and diffuse neutron-scattering data⁴ the PT in RbSCN is very close to the tricritical point. In the compressible pseudospin model the elastic-dipolar interactions are accounted for by a single parameter A .⁵ It can be shown that for $A < \frac{1}{3}$ ($> \frac{1}{3}$) the PT is of second order (first order), whereas for $A = \frac{1}{3}$ the system displays tricritical behavior. For KSCN, $A = 0.44$ was found, whereas for RbSCN $A = 0.35$.² Moreover, from a power-law fit of the temperature dependence of the superstructure Bragg peaks below T_c , $I_B(q_c) \sim \eta^2(T) \sim (T_c - T)^{2\beta}$, a value of $\beta = 0.25$ was found for RbSCN as expected for a tricritical point. The previous investigations demonstrate that in these systems a strong coupling between the orientational degrees of freedom of the SCN molecules (η -order parameter) and the lattice strains (ε_i for $i=1,2,3$) occurs. This strong coupling that due to symmetry is of the type $\sim \eta^2 \varepsilon_i$ ($i=1,2,3$), leads to large anomalies in the longitudinal elastic constants at T_c .⁶ From the dispersion of the longitudinal acoustic modes we obtained an estimation of the order parameter relaxation time $10^{-7} \text{ s} < \tau_\eta < 10^{-3} \text{ s}$ below T_c . Quite recently the slow dynamics of the SCN fluctuations was also detected by ¹⁴N NMR.⁷ A thermally activated temperature dependence of the head-tail flipping rate of SCN molecules was found with $\tau_0 = 3.8 \times 10^{-15} \text{ s}$ and $E = 0.66 \text{ eV}$, implying $\tau = 8 \times 10^{-7} \text{ s}$ at $T_c = 415 \text{ K}$.

The dynamics of the order-parameter fluctuations is also rather slow above T_c . Indeed neutron-scattering experiments in KSCN (Ref. 8) and RbSCN (Ref. 4) yielded that the high-temperature tetragonal phase consists of orthorhombic short-range-ordered clusters that appear static on the neutron-scattering time scale (10^{-11} s). Above T_c the diffuse neutron-scattering intensity of KSCN and RbSCN near the

$\mathbf{q}_c = (100)$ superlattice point obeys a Lorentzian line shape. The correlation length ξ_x (average cluster size) determined from the fits varies from $\xi_x(T_c + 25 \text{ K}) \approx 12 \text{ \AA}$ to $\xi_x(\approx T_c) \approx 40 \text{ \AA}$ for KSCN and $\xi_x(T_c + 20 \text{ K}) \approx 40 \text{ \AA}$ to $\xi_x(\approx T_c) \approx 130 \text{ \AA}$ for RbSCN. The fluctuations are rather isotropic, i.e., $\xi_x = \xi_y \approx 1.6\xi_z$ for KSCN and $\approx 1.4\xi_z$ for RbSCN, respectively. Both, the correlation length ξ and the diffuse intensity $I_D(q_c)$ follow mean-field critical behavior above T_c .

Below T_c the situation is more complex, as previous diffuse neutron-scattering measurements have shown. To clarify the nature of the fluctuation behavior as well as the development from long-range order ($T < T_c$) to short order ($T > T_c$), we have performed a detailed diffuse neutron-scattering study in the ordered phase (below T_c). The results are compared with molecular-dynamics simulations.

II. EXPERIMENT

The measurements were done on the triple-axis spectrometer VALSE, located at a cold neutron guide position of the Laboratory Léon Brillouin at Saclay. The incident neutron energy was 14.7 meV. A pyrolytic graphite filter was put into the incident beam in order to eliminate the higher-order contamination. Pyrolytic graphite PG(002) crystals were used as monochromator and analyzer, respectively. Single crystals of KSCN with a mosaic spread of 20 min were used as samples. The diffuse neutron-scattering investigation was performed from room temperature up to 415 K.

III. DIFFUSE SCATTERING RESULTS

The measurements were done in the neighborhood of the (100), (200), and (300) points in the (a^*, b^*) plane of the reciprocal lattice of the orthorhombic phase, performing longitudinal ($h + q_x, 0, 0$) and transverse ($h, q_y, 0$) scans. The (100) and equivalent points are superlattice points (\mathbf{q}_c) related to the antiferrodistortive configuration of the SCN molecules in the ordered phase.²

At room temperature a sharp Bragg reflection above a flat background was observed, implying that the crystal is in the long-range-ordered state. The first significant changes in the scattering pattern occurred at $T \approx 400 \text{ K}$, i.e., about 15 K below T_c , where the sharp superlattice reflections showed an

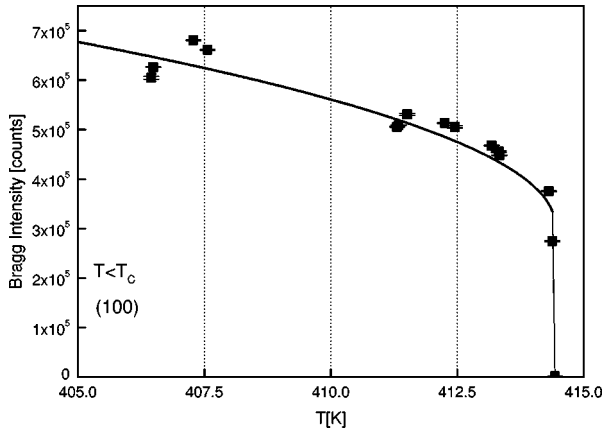


FIG. 1. Temperature dependence of the Bragg intensity at the superlattice positions $\mathbf{q}_c = (100)$. The solid line represents a guide to the eye.

intensity decrease and a broad intensity distribution appeared, which was centered at the superlattice points. On further heating, the Bragg intensity of the superlattice reflections decreased (Fig. 1). Simultaneously, the diffuse scattering intensity increased significantly when heating towards T_c . Figure 2 shows the change of the diffuse scattering around the (100) point in longitudinal and transverse scans for several temperatures below T_c . Similar behavior was found in the vicinity of the (300) wave vectors.

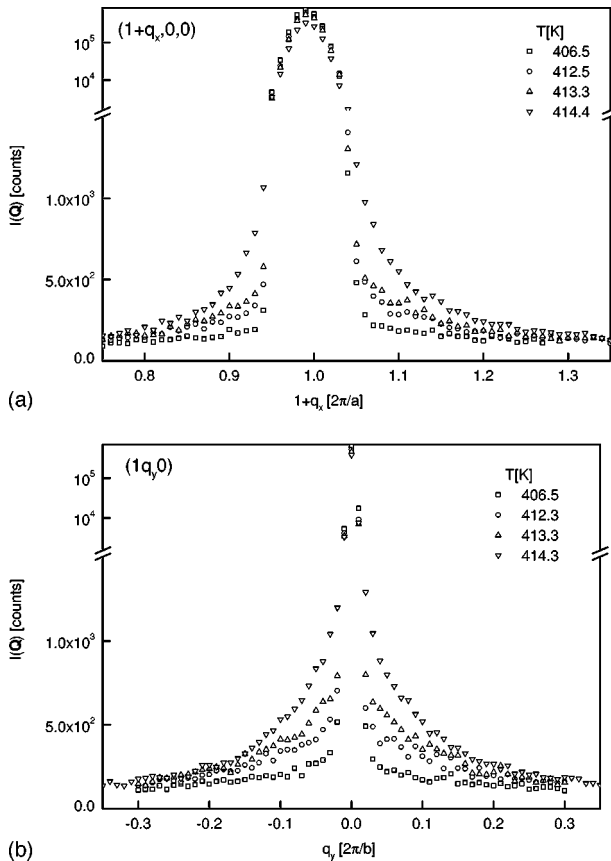


FIG. 2. Diffuse scattering intensity measured in the vicinity of the superlattice points (a) for longitudinal scans $\mathbf{q} = (1 + q_x, 0, 0)$ and (b) for transverse scans $\mathbf{q} = (1, q_y, 0)$.

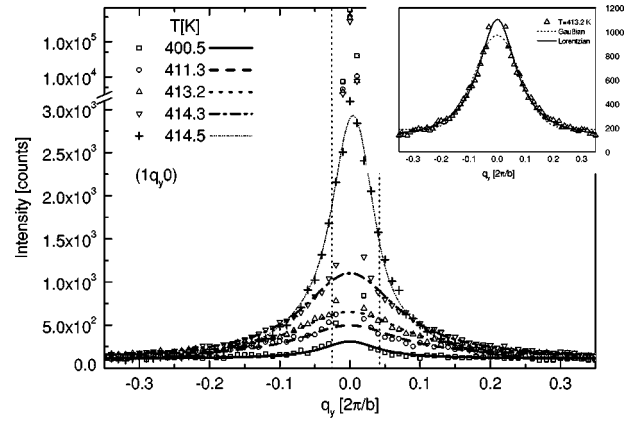


FIG. 3. Diffuse scattering intensities fitted with a Lorentzian line shape (see text). The inset shows a comparison between Lorentzian and a Gaussian fitting function.

IV. DATA EVALUATION

In our previous works^{8,9} we found that the diffuse scattering in the orthorhombic phase of KSCN can be well described by a Gaussian function, and we concluded that the diffuse neutron scattering below T_c is due to the presence of small-sized microdomains of various orientations. Since the present data have been collected on a finer temperature mesh and on a larger sample, the quality of the diffuse scattering results is much better compared to our previous results, i.e., the intensity of the diffuse scattering is an order of magnitude higher (compare, e.g., Ref. 8). This allowed us to analyze the data in the orthorhombic phase in more detail.

To clarify the origin of the diffuse scattering below T_c , we tried fitting the whole data set at different temperatures for the $(1 + q_x, 0, 0)$, $(1, q_y, 0)$, $(3 + q_x, 0, 0)$, and $(3, q_y, 0)$ wave vectors with various line shapes: (a) Gaussian, (b) square of the Fourier transform of a box function (both corresponding to small-sized microdomains), (c) different distribution functions (corresponding to distributions of domain sizes), (d) Lorentzian (corresponding to thermal order-parameter fluctuations), (e) discrete version of Lorentzian.¹⁰ It turned out that the best fits for all data could be obtained with the discrete Lorentzian and the Lorentzian intensity dis-

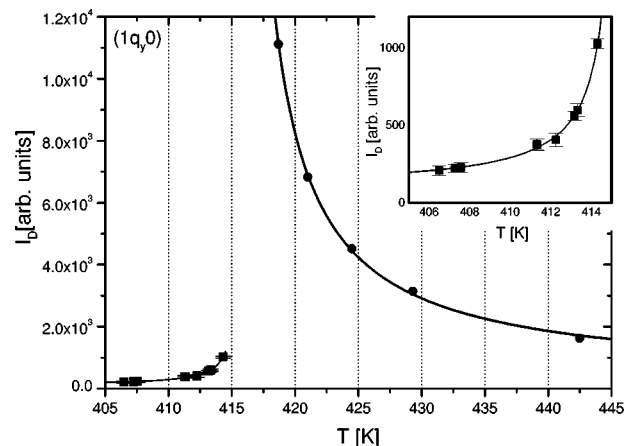


FIG. 4. Temperature dependence of the diffuse scattering intensity at \mathbf{q}_c . The solid line above T_c represents the mean-field results (Ref. 2). The line below T_c is a guide to the eyes.

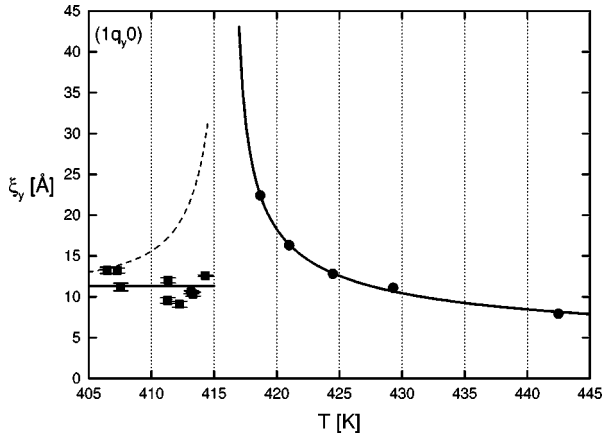


FIG. 5. Temperature dependence of the correlation length of the order parameter fluctuations. The dashed line was calculated according to Eq. (1), i.e., $\xi(T) \sim \sqrt{I_D(q=0)}$. The solid line above T_c is obtained from the fit using the mean-field equations (Ref. 2).

tributions (Fig. 3), i.e., both functions fit equally well. The Lorentzian line shape implies that the diffuse scattering below T_c is due to the appearance of order-parameter fluctuations as a precursor to the order-disorder PT. Figure 4 shows as an example the diffuse scattering intensity $I_D(\mathbf{q}_c)$ and in Fig. 5 the correlation length $\xi_y = 1/w_y$ (where w_y is the half width at half maximum of the diffuse intensity) as a function of temperature is displayed. It is a striking feature that the diffuse intensity increases strongly when approaching T_c from both sides, whereas the correlation length remains constant below T_c .¹¹ The same behavior was also found for the q_x and the q_z direction. The whole problem becomes even more transparent if one applies simple Landau-Ginzburg theory. In this theory the Lorentzian line shape of the diffuse intensity follows from an exponential decay of the two-point correlation of the order-parameter fluctuations and the diffuse intensity is given as¹²

$$I_D(\mathbf{q}) = |G(\mathbf{q})|^2 \frac{k_B T \xi^2}{1 + q_x^2 \xi_x^2 + q_y^2 \xi_y^2 + q_z^2 \xi_z^2}, \quad (1)$$

where $G(\mathbf{q})$ is the structure factor, \mathbf{q} is the wave vector with respect to the peak position at the superlattice points (\mathbf{q}_c), and $\xi = |(\xi_x, \xi_y, \xi_z)|$, with ξ_x, ξ_y, ξ_z are the correlation lengths of the order-parameter fluctuations in three corresponding directions. According to Eq. (1), $I_D(q=0, T) \sim \xi^2(T)$, which below T_c is in contrast with our experimental findings (Figs. 4 and 5). Above T_c the relation $I_D(q=0, T) \sim \xi^2(T)$ is nicely fulfilled and both quantities are well described by a mean-field critical behavior,⁹ i.e., $\xi_x^+ = \xi_y^+ = 65.8 \text{ \AA} / \sqrt{T - T_0}$, $\xi_z^+ = 41.7 \text{ \AA} / \sqrt{T - T_0}$, and $I_D^+ = I_0 / (T - T_0)$, where $T_0 = T_c - 2.5 \text{ K}$ as the phase transition is of first order.

V. COMPARISON WITH MOLECULAR-DYNAMICS SIMULATIONS

To obtain some insight into processes occurring close to T_c in the MSCN family of crystals we have done molecular-dynamics simulations of a two dimensional KSCN model. In fact, we employed the model defined previously.^{13,14} Let us

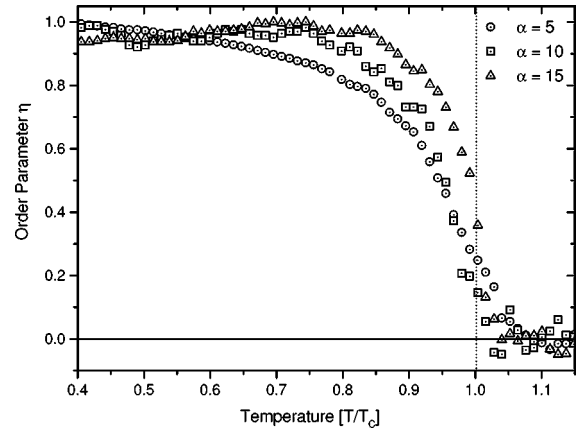


FIG. 6. Calculated temperature dependence of the orientational order parameter η for different strengths of the order-parameter-strain coupling α .

briefly recapitulate its properties. The model is two dimensional consisting of two kinds of particles. One of them represents potassium ions, that have translational degrees of freedom. These particles interact via aharmonic potential with nearest and next nearest neighbors. The second kind of particles possesses rotational degrees of freedom and represents the SCN molecules. Each of the particles of this kind resides in a local anharmonic potential that is of fourth order and invariant with respect to the point group of the high-temperature phase ($I4/mcm$) of KSCN. The configuration of both kinds of particles is described by two different order parameters. One that we call ε is connected to the strain in the potassium sublattice. The other order parameter η describes the orientation of the particles of the SCN sublattice. In the Hamiltonian of the model there is a term that due to symmetry is of the form $\alpha \eta^2 \varepsilon$. It corresponds to the order-parameter-strain interaction of the compressible pseudospin model. The full details of the model are presented in Refs. 14 and 13.

To study the role of the elastic forces in such kinds of models, we performed simulations for different values of the coupling constant α . We used systems of 110×110 unit cells with free boundary conditions. Equations of motion

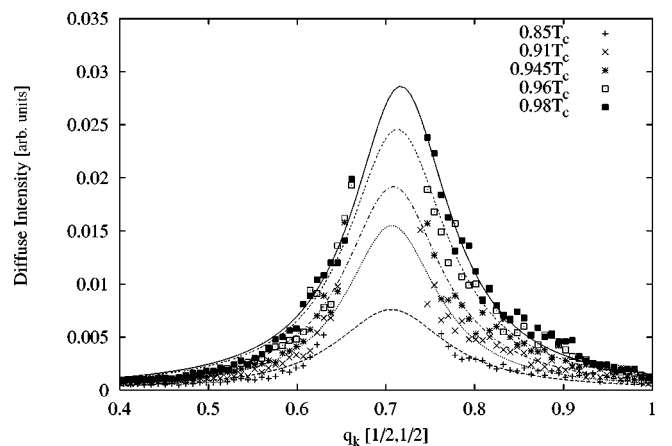


FIG. 7. Calculated temperature and wave-vector dependences of the diffuse scattering intensities for a system with $\alpha = 15$. The lines represent fits with Lorentzian line shapes.

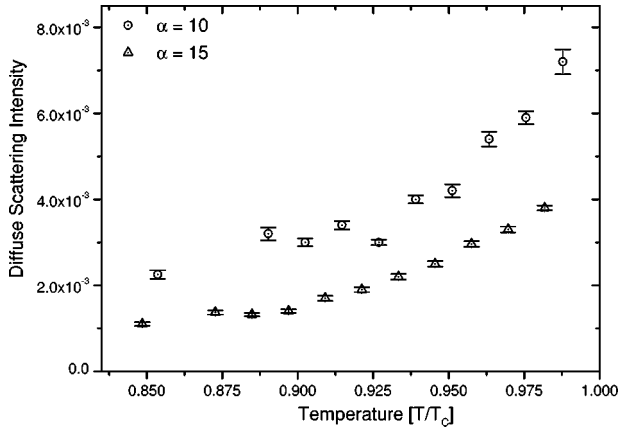


FIG. 8. Calculated temperature dependence of the diffuse intensity at \mathbf{q}_c for two values of α . Data were obtained from the Lorentzian fits shown in Fig. 7.

were integrated by the symplectic central difference method and the Gaussian thermostat was applied as canonical procedure.¹⁵ Wave-vector-dependent properties were calculated by the standard formula for kinematic scattering, with straightforward Fourier transformation that is assumed to be optimal for this kind of problem.¹⁶ Each calculation was done under the same conditions on 40 independent initial configurations followed by an averaging of the results.

Figure 6 presents the calculated temperature dependence of the orientational order parameter for different values of the coupling constant α . We observe that with increasing value of α the slope of the order parameter becomes steeply close to T_c , in agreement with simple mean-field theory.² The observed smearing of the PT is due to finite-size effects.

Figure 7 shows as an example diffuse scattering peaks for $\alpha = 15$. Note that the peak is centered at $|\mathbf{q}| = 1/\sqrt{2}$, which results from the different orientation of the unit-cell in our model¹³ as compared with the unit cell orientation of real KSCN. Similar to the experimental data, the calculated diffuse intensity can be well fitted by a Lorentzian. From the fits we obtained the diffuse intensity at the critical wave vector and the correlation length of the order-parameter fluctuations for various coupling constants α and temperatures. The results are presented in Figs. 8 and 9.

The simulations clearly show the same features as compared with the experimental data on the diffuse scattering. For strong order-parameter–strain coupling the diffuse intensity increases when approaching T_c from below, whereas the correlation length ξ remains constant throughout the orthorhombic phase. For a similar model (four-states Potts model) without order-parameter–strain coupling ($\alpha = 0$) both $I(\mathbf{q}_c)$ and ξ increase strongly when approaching T_c from below, as is known from the theory of critical phenomena. Previous molecular-dynamics calculations have shown, that in the high-temperature phase, both the diffuse intensity and the correlation length show a divergent behavior even for a

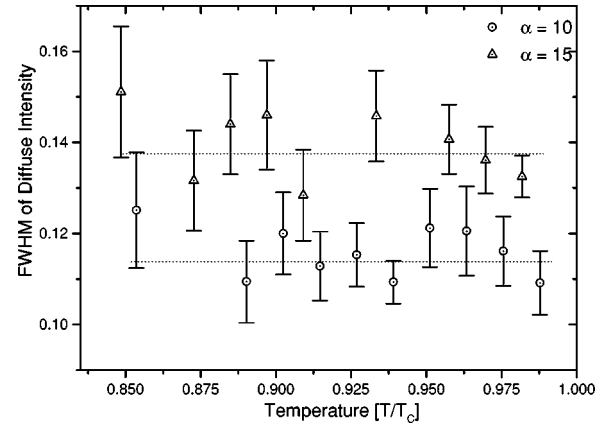


FIG. 9. Calculated temperature dependence of the full width at half maximum (FWHM $\sim \xi^{-1}$) for different coupling constants α . Data were obtained from the Lorentzian fits shown in Fig. 7.

strong coupling between the order parameter and the strain,¹⁴ in agreement with the experimental findings (Figs. 4 and 5).

VI. SUMMARY

The present refined experimental data yielded new insight into the nature of the order-disorder phase transition in KSCN. In contrast to our previous work,^{8,9} we were able to detect a strong increase of the diffuse intensity (critical scattering) when approaching T_c from the low-temperature phase. However, interestingly enough the width of the diffuse scattering intensity remains constant below T_c . This is a surprising result, since in any simple model, the temperature dependences of the diffuse intensity $I_D(\mathbf{q}_c)$ and its width $\sim \xi^{-1}$ are coupled. That is, in the simplest Landau-Ginzburg theory $I_D(\mathbf{q}_c) \sim \chi(\mathbf{q}_c, T) \sim \xi^2(T)$, which follows from the fact that $\chi(\mathbf{q}_c) = 1/(k_B T) \int dV' G(\mathbf{r}, \mathbf{r}') = \xi^2/C$ for an exponential decay of the order-parameter fluctuations. Indeed, this relation between the diffuse intensity and the correlation length is nicely fulfilled in the high-temperature phase of KSCN,² but is violated below T_c .

As we have shown by molecular-dynamics simulations, below T_c the correlation length of the order-parameter fluctuations can be stabilized by elastic strain interactions. To understand the role of the elastic forces in more detail we are working on an analytic theory, which is based on a Landau-Ginzburg model including coupling between order parameter and strain, and a perturbative calculation of the two-point correlation function of the order-parameter fluctuations.¹⁷

ACKNOWLEDGMENTS

The present work was supported by the Fonds zur Förderung der wissenschaftlichen Forschung in Austria (Project No. P 12226-PHY). We are indebted to Dr. A. Fuith for supplying the large high-quality KSCN single crystals. One of the authors (Z.Ł.) would like to acknowledge the great hospitality during his stay at the University of Vienna.

*Deceased.

[†]On leave from the Institute of Nuclear Physics, ul. Radzikowskiego 152, 31-342 Krakow, Poland.

¹A. Fuith, Phase Transit. **62**, 1 (1997).

²W. Schranz, Phase Transit. **51**, 1 (1994).

³W. Schranz, A. Fuith, and Z. Łodziana (unpublished).

⁴O. Blaschko, W. Schwarz, W. Schranz, and A. Fuith, J. Phys.: Condens. Matter **6**, 3469 (1994).

- ⁵W. Schranz, H. Warhanek, R. Blinc, and B. Žeks, *Phys. Rev. B* **40**, 7141 (1989).
- ⁶W. Schranz and D. Havlik, *Phys. Rev. Lett.* **73**, 2575 (1994).
- ⁷R. Blinc, T. Apih, A. Fricelj, J. Dolinsek, J. Seliger, A. Fuith, W. Schranz, H. Warhanek, and D. C. Ailion, *Europhys. Lett.* **39**, 627 (1997).
- ⁸O. Blaschko, W. Schwarz, W. Schranz, and A. Fuith, *Phys. Rev. B* **44**, 9159 (1991).
- ⁹O. Blaschko, W. Schwarz, W. Schranz, and A. Fuith, *Ferroelectrics* **124**, 139 (1991).
- ¹⁰S. Singh and A.M. Glazer, *Acta Crystallogr., Sect. A: Cryst. Phys., Diffr., Theor. Gen. Crystallogr.* **A37**, 804 (1981).
- ¹¹This behavior is independent of the used fitting function.
- ¹²B. Dorner and R. Comès, in *Dynamics of Solids and Liquids by Neutron Scattering*, edited by S.W. Lovesey and T. Springer (Springer-Verlag, Berlin, 1977), p. 159.
- ¹³K. Parliński, *Phys. Rev. B* **50**, 59 (1994).
- ¹⁴Z. Lodziana and K. Parliński, *Phase Transit.* **58**, 273 (1996); *Ferroelectrics* **191**, 65 (1997).
- ¹⁵S. Hess, in *Computational Physics*, edited by K.H. Hoffmann and M. Schreiber, Springer Series in Computational Physics, (Springer, Berlin, 1996).
- ¹⁶B.D. Butler and T.R. Welberry, *J. Appl. Crystallogr.* **25**, 391 (1992).
- ¹⁷A. Tröster and W. Schranz (unpublished).